Plastic hinge models for the seismic assessment of reinforced concrete wall-type piers with detailing deficiencies

P. Hannewald & K. Beyer
École Polytechnique Fédérale Lausanne, Switzerland

SUMMARY:
Plastic hinge models are widely used in earthquake engineering to predict the load-deformation relationships of reinforced concrete members. For the seismic assessment of bridges, it is appealing to use those relatively simple models if the response is predicted with sufficient accuracy. The applicability of these models to wall-type bridge piers with weak seismic detailing is examined. Flexural and shear deformations were computed using several approaches and the results were compared with experimental data of such piers. A couple of modelling approaches exist that allow accounting for shear deformations, which are not negligible for wall-type piers, within the scope of plastic hinge analysis. Computing the shear deformations was associated with considerable scatter while the flexural deformations were generally predicted well. The paper concludes with identifying those assumptions underlying the shear deformation models, which differ from the experimental observations and should therefore be modified if applied to the examined type of structures.

Keywords: RC bridge piers, plastic hinge analysis, detailing deficiencies, shear deformations

1. INTRODUCTION

For the seismic assessment of reinforced concrete (RC) bridges in engineering practice it is desirable to employ comparatively simple mechanical models with which the load-deformation behaviour of the structure can be predicted with sufficient accuracy. A widely used approach is the plastic hinge modelling whose applicability for the analysis of wall-type bridge piers is examined in this paper. This is done based on experimental data from a test campaign conducted at ETH Zurich, where this type of pier has been tested in 1:2 scale under quasi-static cyclic loading. These piers were representative of existing bridge piers in Switzerland which were not designed according to modern seismic design guidelines.

Firstly, a brief overview of the test campaign is presented in this paper, in which some of the focal points and results which are necessary for the modelling will be highlighted. Then, an overview of commonly employed plastic hinge length equations for walls is presented along with approaches to include the shear deformations in the modelling. In the following section, the results obtained by employing the previously introduced approaches are compared to the experimental data. Finally, some conclusions regarding the applicability of the examined modelling approaches are drawn.

2. EXPERIMENTAL DATA

2.1 Layout of test units and test setup

A series of seven quasi-static cyclic tests on wall-type cantilever RC bridge piers, tested in the structural engineering laboratory of the ETH Zurich, were analysed. The test units were to be representative of existing piers in Switzerland designed according to codes without seismic provisions

and therefore constructed with little transverse reinforcement, which was not anchored in the core concrete, as well as spliced reinforcement in the plastic region at the pier base. For further information on the choice of the pier characteristics as well as on part one of the test series (VK1-VK3) the reader is referred to Bimschas (2010). All test units had a rectangular cross section with dimensions $b = 0.35$m and $l_w = 1.50$m. The longitudinal reinforcement, which consisted of ductile reinforcing bars with $d_l = 14$mm diameter, was evenly distributed along the circumference of the cross section. In Table 2.1 some of the main characteristics of the test units are summarised. A cyclic loading history with two cycles at each force or displacement level, small intermediate cycles in the inelastic range and constant normal force was applied to all test units. Measurements of vertical elongations along the narrow faces of the test units as well as of horizontal displacements were taken by means of LVDTs. Deformations of the surface were measured along a square grid using an optical system or demountable displacement transducers, respectively. Further information on the test setup, measurements and results can be found elsewhere (Bimschas, 2010; Hannewald et al., 2012), hence only some results, which were needed to evaluate the quality of the predictions, are reported in the following section.

Table 2.1 Properties of analysed test units

Test unit	**VK1**	**VK2**	**VK3**	**VK4**	**VK5**	**VK6**	**VK7**
Shear span L_s	3.30m	3.30m	3.30m	3.30m	4.50m	4.50m	3.30m
Aspect ratio L_s/l_w	2.20	2.20	2.20	2.20	3.0	3.0	2.20
Concrete strength f_c	39.0MPa	35.0MPa	34.0MPa	34.6MPa	35.2MPa	44.4MPa	30.0MPa
Steel strength f_y	521MPa	521MPa	521MPa	521MPa	521MPa	521MPa	521MPa
Axial load ratio	0.064	0.071	0.073	0.072	0.070	0.056	0.083
Reinforcement ratios	0.82%	0.82%	1.23%	1.23%	1.23%	1.23%	1.23%
long. / transv.	0.08%	0.08%	0.08%	0.08%	0.08%	0.08%	0.22%
Lap splice length	-	$l = 43d_l$	-	$l = 43d_l$	$l = 43d_l$	-	-

2.2 Test results

The objective of a plastic hinge analysis is to predict the force-deformation envelope of a structural member and not the complete cyclic response. Therefore, only the envelope of the cyclic response, shown in Figure 2.1 is of interest in this study. Since the elastic and inelastic parts of the response are clearly distinguished in the plastic hinge modelling, the measured response is plotted against the displacement ductility. The latter was defined related to the experimentally determined nominal yield displacement as suggested by Priestley et al. (2007). As mentioned previously, the shear deformations cannot be neglected for wall type structures. Usually they are accounted for by means of their ratio to the flexural deformation, which was often observed to be constant in the inelastic range, if the behaviour of the walls was dominated by flexure (e.g. Dazio et al., 2009; Beyer et al., 2011). For this reason, the ratio of the shear to flexural deformations, plotted against ductility, is also presented in Figure 2.1. The deformation components were determined from the measurements of the outer columns of the grid points on the surface of the test units. The displayed shear deformations contain the deformation due to base sliding and the flexural deformations contain the component due to anchorage slip of the reinforcement bars out of the foundation. Note that once an accelerated degradation sets in, displacement components were no longer determined, because some measurement points at the base, where the concrete was severely damaged at that time, were missing.

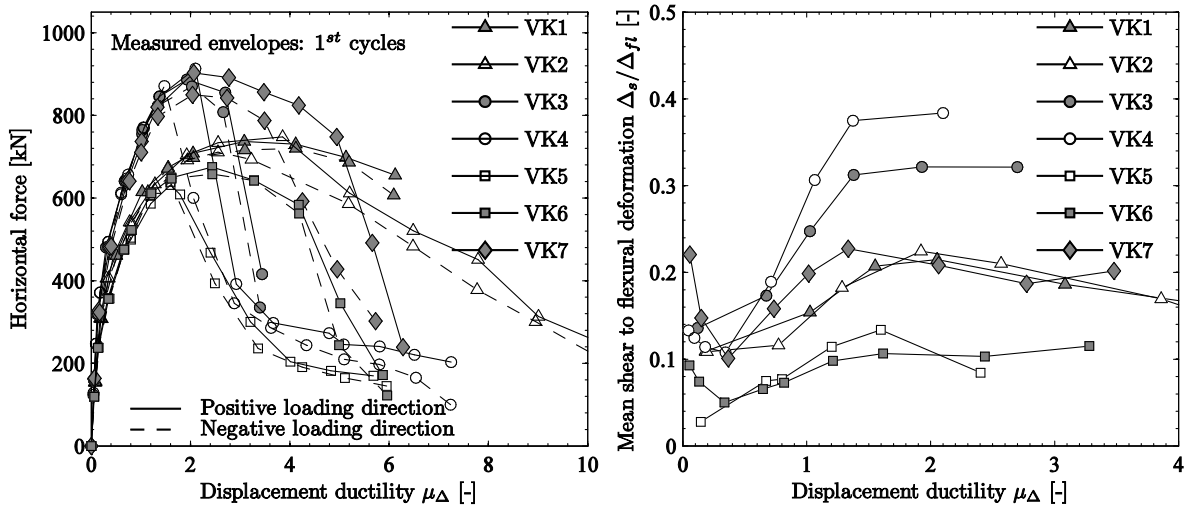

Figure 2.1 Experimentally determined force-deformation envelopes at first cycles to the left and average shear to flexural deformation ratios from positive and negative first cycle loading to the right.

3. PLASTIC HINGE MODELS FOR WALLS

3.1 Overview of plastic hinge lengths

Some more recent propositions for plastic hinge lengths L_p have been employed as well as those included in the current Eurocode EC8 on seismic design. In Annex A of EC8 Part 3 (CEN, 2005) a plastic hinge length, in which the member geometry, tension shift and strain penetration components are included, is recommended:

$$L_p = \frac{L_s}{30} + 0.2l_w + 0.11\,\frac{d_l f_y}{\sqrt{f_c}} \tag{3.1}$$

With this length and the strain limits as defined in (CEN, 2005) the ultimate displacement of the member is supposed to be determined. The same components are included in the proposal by Priestley et al. (2007) but with partially different factors. The first component was assumed to account for the spread of plasticity along the member and was hence chosen dependent on the ratio of ultimate to yield strength of the reinforcement steel. To account for tension shift, the same term as in Eqn. (3.1) is included if the mean response is to be computed ($0.2l_w$); for a more conservative deformation estimate the authors recommend using half that length ($0.1l_w$). For the strain penetration component a term in which only the longitudinal bar diameter d_l and the reinforcement yield strength f_y are included is suggested. The plastic hinge length is then calculated as follows:

$$L_p = \min\left(0.2\left(\frac{f_u}{f_y} - 1\right), 0.08\right) L_s + 0.2l_w + 0.022\, f_y d_l \tag{3.2}$$

Biskinis and Fardis (2010a) proposed plastic hinge lengths which foremost depend on the type of loading that is applied. Based on a large experimental database, which comprised also test units with a rectangular wall-type cross section, they proposed plastic hinge lengths with which the ultimate rotation was captured best on average. This empirical investigation led, for structural members with good seismic detailing, to the following proposed plastic hinge length equation, which is merely dependent on the member geometry:

$$L_{p,cyc} = 0.2l_w\left(1 + \frac{1}{3}\min\left(9, \frac{L_s}{l_w}\right)\right) \tag{3.3}$$

Note that no proposal for cyclic loading in combination with poor seismic detailing is made. To explicitly derive a plastic hinge length for walls with rectangular cross section, Bohl and Adebar (2011) conducted a numerical study employing the modified compression field theory and proposed plastic hinge length equations based on the observed spread of inelastic strains in the model. The inelastic strains were found to be linearly distributed over the height over which plasticity spreads and the proposed plastic hinge length corresponds to half this height. Originally, one of the objectives of the study was to examine the influence of shear stress on L_p. From the numerical results Bohl and Adebar concluded that the shear stress was sufficiently accounted for by including both the wall length l_w and shear span L_s in the equation but that the axial load ratio should explicitly be considered:

$$L_p = (0.2l_w + 0.05L_s)\left(1 - 1.5\frac{P}{A_g f_c}\right) \leq 0.8l_w \tag{3.4}$$

where P is the axial load and A_g the gross cross sectional area. According to Bohl and Adebar, this length should serve as a lower bound limit of an isolated cantilever. To compare the recommended values for L_p with the experimental data, the following procedure by Hines et al. (2004) is employed to determine an estimate of the plastic hinge length from the experimental data. This estimate corresponds to the length which – in conjunction with the plastic base curvature ϕ_p – yields the observed plastic flexural deformation. The plastic base curvature ϕ_p is computed by subtracting the elastic curvature from the extrapolated total curvature at the base ϕ_b. The latter is assumed to be the curvature at the wall base for a linear least square error fit of the plastic curvature profile near the pier base. To minimise the influence of potentially unsymmetrical crack patterns it is recommended to fit average curvature profiles from positive and negative loading direction. Using the plastic flexural deformation $\Delta_{p,fl}$, which can be determined from measurement data, the plastic hinge length necessary to predict those deformation in conjunction with the plastic base curvature ϕ_p can be calculated as:

$$L_p = \frac{\Delta_{p,fl}}{\phi_p L_s} \tag{3.5}$$

The difference between ϕ_b and the curvature obtained from measurements is interpreted as strain penetration influence. If the strain penetration influence is assumed to be a linear relation between plastic curvature and strain penetration length, the latter can be determined as follows:

$$L_{sp} = L_{b,m}\left(\frac{\phi_{b,m}}{\phi_b} - 1\right) \tag{3.6}$$

where $L_{b,m}$ is the baselength of the measurement device which crosses the base crack, and $\phi_{b,m}$ the average curvature determined from the measurements of the device with the baselength $L_{b,m}$. The plastic hinge length without strain penetration component can then be obtained by subtracting the strain penetration component determined with Eqn. (3.6) from the plastic hinge length computed with Eqn. (3.5).

3.2 Shear deformations

Based on the observation that the ratio of shear to flexural deformation Δ_s/Δ_{fl} remained approximately constant in the inelastic displacement range, provided that the shear capacity did not significantly degrade, models accounting for the shear deformation were developed by Hines et al. (2004) and Beyer et al. (2011). The first was derived based on kinematic considerations with the assumption that all shear deformations stem from a region framed by two cracks, along which inelastic strains occur. For the lower crack a 60° angle was suggested while the angle of the upper crack θ_m was determined from force equilibrium at the crack face. Furthermore, it was assumed that 35% of all flexural deformations originate in that same region and that the shear deformations increase if the walls have little transverse reinforcement or thin webs. This effect was accounted for with an empirical factor α, which relates the shear force to the capacities defined by web crushing and diagonal tensile strength. The proposed equation is (Hines et al., 2004):

$$\frac{\Delta_s}{\Delta_{fl}} = 0.35(1.6 - 0.2\theta_m)\frac{L_s}{l_w}\alpha \quad (3.7)$$

Beyer et al. (2008) observed that with this estimate good predictions were obtained if the axial force of the section was not in tension. To include the axial load level, a model was developed in which shear strains were related to axial strains ε_x based on Mohr's circle, with the assumption that the angle of the principal strains corresponds to the crack angle θ (Beyer et al., 2011). As a simplification, it was assumed that both shear and flexural deformations occur only inside the plastic hinge region and can thus be related using the curvature ϕ:

$$\frac{\Delta_s}{\Delta_{fl}} = 1.5\frac{\varepsilon_x}{\phi \tan\theta}\frac{1}{L_s} \quad (3.8)$$

4. APPLICATION OF PLASTIC HINGE MODELS

4.1 Flexural response

Table 4.1 summarizes the predicted plastic hinge lengths according to Equations (3.1) to (3.4) as well as the plastic hinge length derived from experimental measurements (Eqn. (3.5)). Only test units without lap splices are included in Table 4.1. The curvature profile of the test units with lap splices was not linear at the base (Bimschas, 2010; Hannewald et al., 2012) and therefore the equivalent plastic hinge length could not be determined with the approach underlying Eqn. (3.5). Note that the Equations (3.1) to (3.4) for predicting plastic hinge lengths do not distinguish between walls with and without lap splice. The predicted values for walls with lap splice at the base would therefore be – apart from small variations due to slightly different concrete strength values f_c – identical to those for the test units without lap splice. Note that the equations for the plastic hinge length vary with regards to whether or not strain penetration is included. For example, Biskinis and Fardis (2010) do not include the strain penetration term in the plastic hinge length equation but add the deformation due to strain penetration as a separate component when calculating the flexural response . Hence, the plastic hinge lengths predicted with Eqn. (3.3), proposed by Biskinis and Fardis, as well as Eqn. (3.4), proposed by by Bohl and Adebar, do not contain a strain penetration component, whereas all others do, including the plastic hinge lengths derived from experimental data (Eqn. (3.5)). The evaluation of the experimental data yielded decreasing plastic hinge lengths with increasing ductility, hence a range of values is given in the last column of Table 4.1.

Table 4.2 Estimated plastic hinge lengths in mm.

	Predicted plastic hinge lengths				**L_p from experimental data**
Test unit	**Eqn. (3.1)**	**Eqn. (3.2)**	**Eqn. (3.3)**	**Eqn. (3.4)**	**Eqn. (3.5)**
VK1	538	599	520	419	365 – 977
VK4	548	599	520	412	326 – 653
VK6	570	612	600	479	354 – 628
VK7	556	572	520	405	329 – 644

To determine the force-deformation relationship based on plastic hinge analysis, moment-curvature analyses were carried out on cross sections with zero length fibre elements using Matlab (2010). The reinforcement was modelled using a bilinear constitutive law including strain hardening and for the concrete the model for confined concrete according to Mander et al. (1988) was applied. With these material models, good agreement between numerically predicted moment-curvature relationships and those determined from the LVDT readings was achieved. The flexural response of the test units was estimated according to the formulations recommended by the authors of the various plastic hinge lengths. If no recommendations for the calculation of the flexural response were provided (L_p

according to Eqn. (3.4)) the response was calculated according to the refined model by Priestley et al. (2007). The predictions of the global force-deformation response as well as the prediction of the flexural deformation for a given compression strain level in the plastic hinge region were compared with the experimental data. Figure 4.1 shows the predicted and measured flexural responses, including the predictions of the deformation for a certain strain limit, of two of the test units with continuous reinforcement. The flexural deformations at which concrete compressive strains of $\varepsilon_c = 0.0046$ (VK6) and $\varepsilon_c = 0.004$ (VK7) were reached are marked with circles in the predicted curves and with additional markers for the experimental data. The first corresponds to the ultimate strain calculated according to Biskinis and Fardis (2010a), while for the second $\varepsilon_c = 0.004$ was marked because the computed ultimate strain ($\varepsilon_c = 0.0086$) was outside the range measureable with the LVDTs.

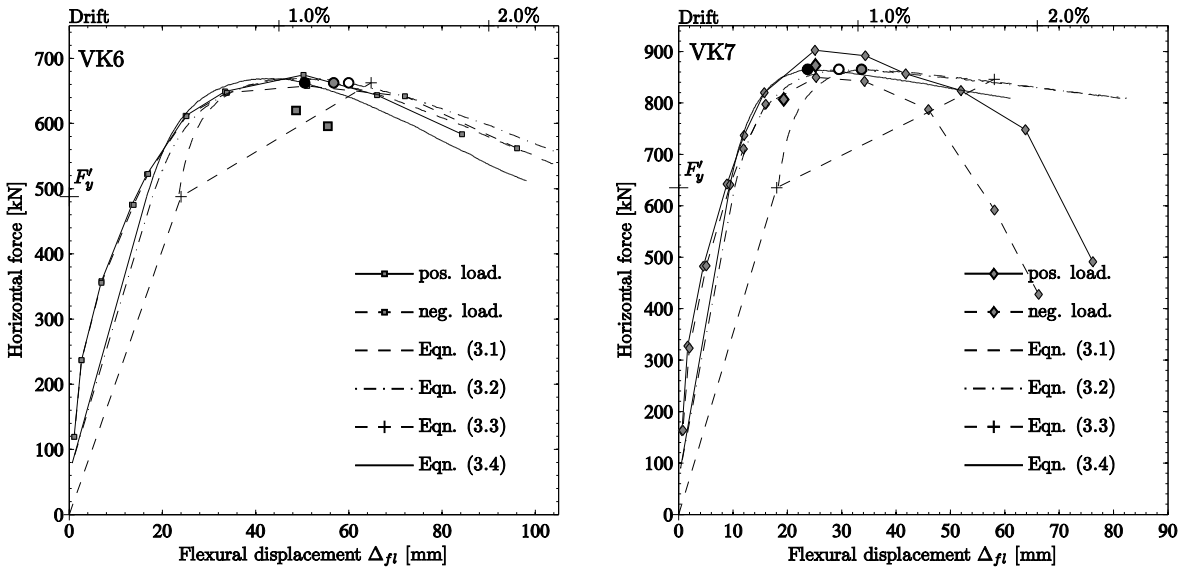

Figure 4.2 Experimentally determined force- flexural-deformation envelopes at first cycles and predictions. Points corresponding to concrete strains of 0.0046 (VK6) and 0.004 (VK7) are marked with circles.

One can see that the overall predictions match the experimentally determined response generally reasonably well. An exception is the prediction of the yield displacement according to the EC8 approach (CEN, 2005) and the approach by Biskinis and Fardis (2010b) which are used in combination with L_p according to Eqns. (3.1) and (3.3), respectively. These approaches considerably overestimate the observed yield displacement. It is believed that this is related to the shear deformation component and the assumed deformation increase due to inclined flexural cracking included in these models – components which are not included in the other models. When L_p of Eqn. (3.2) is employed, deformations are slightly overestimated, which could be changed by using the more conservative recommendation of $0.1l_w$ instead of $0.2l_w$. However, it appears that this way an overestimation of the strain penetration effect is compensated with a reduced tension shift component. The plastic hinge length according to Eqn. (3.4) estimates the experimentally observed relationship between displacement and compression strain rather well. One needs to keep in mind though that it might be difficult to match the strains and corresponding displacements from a monotonic prediction to a cyclic test, which is illustrated, for example, by the prediction of VK6 in Figure 4.1. In this case, the assumed limit strains were first exceeded during a second cycle and on an ascending branch rather than at the peak of a cycle. Hence, the experimentally determined points corresponding to the limit strains are below the envelope and thus below the curve one aims to predict.

4.2 Shear response

The shear to flexural deformation ratio has been estimated according to Eqns. (3.7) and (3.8). For both formulations the crack angles measured in the top part of the test units have been used to eliminate a potential influence of crack angle predictions on the results. For Eqn. (3.7) the measured shear force V

and the web crushing capacity according to EC2 (CEN, 2004) were employed and the curvature needed for application of Eqn. (3.8) has been taken from the section analysis. Figure 4.2 shows the predicted shear to flexural deformation ratios of all test units against the experimentally determined ones at peak load. One can see that the overall agreement is not satisfactory. Especially the ratios of the two test units with the high moment capacity but little transverse reinforcement and aspect ratio 2.2 are not estimated well by any model. The ratios predicted according to Eqn. (3.8) are generally within the range of 20-25% for the shorter test units and around 15% for the longer ones; see Figure 4.2 (b). Ratios predicted with Eqn. (3.7) lie between 10-23%, see Figure 4.2 (a).When the ratios predicted with Eqn. (3.8) are multiplied with the correction factor proposed by Hines et al. (2004) instead of the factor 1.5, the general trend is also captured better, see Figure 4.2 (c). With this modification, the previous Eqn. (3.8) follows to be:

$$\frac{\Delta_s}{\Delta_{fl}} = \alpha \frac{\varepsilon_x}{\phi \tan\theta} \frac{1}{L_s} \tag{4.1}$$

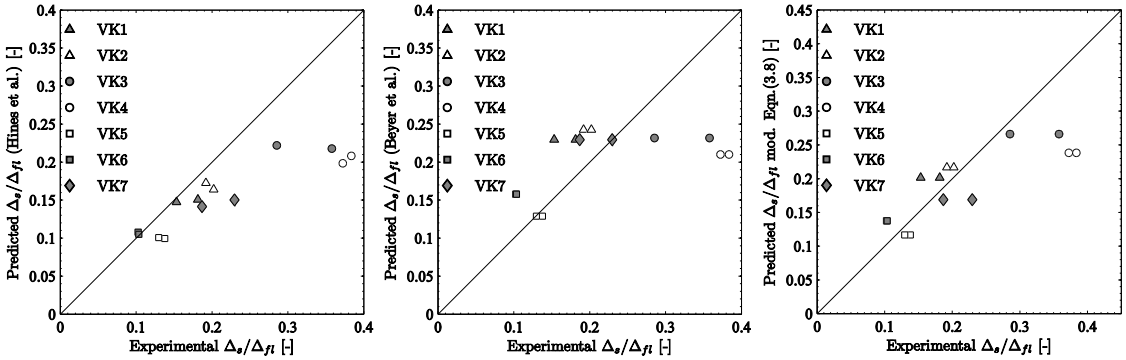

Figure 4.2 Predicted against experimentally determined shear to flexural deformation ratios of all analysed test units at peak load.

The performance of these models hence depends also on the empirically determined correction factors. In both models, crack angles measured from photographs of the test units were used. Predicting feasible crack angles was not possible with the proposed equations. If the equation developed by Hines et al. (2004) is employed with the crack angle corresponding to the spread of plasticity determined according to the procedure outlined in the same publication, the ratios are overestimated. Crack angles predicted according to Bentz et al. (2006) and Collins and Mitchell (1991) were larger than the measured ones and resulted hence in underpredictions of the shear to flexural deformation ratio in combination with Eqns. (3.7) and (3.8). One should also keep in mind that both equations were developed based on some observations and assumptions that do not hold for the analysed data. Contrary to what was assumed by Beyer et al. (2011), the shear deformations did not concentrate in the plastic hinge region, but were distributed rather evenly over the entire cracked height of the test units. Hines et al. (2004) assumed shear deformations also further up the member, but therefore neglected deformations occurring below a 60° crack at the bottom. Furthermore, they observed that roughly 35% of the flexural deformation originates from the considered area between the two cracks, an observation which was not confirmed for the test data examined herein.

5. CONCLUSIONS

With the plastic hinge approaches employed in this study the flexural response was generally predicted in a satisfactory way. Good agreement was obtained for the overall response, also with regards to the predicted deformation corresponding to limit compressive strains, with some of the plastic hinge lengths. At yield, the shear deformations were still small and hence increasing the yield displacement by accounting for shear deformations as well as inclined cracks led to overestimation of the

deformation. No satisfactory agreement was obtained concerning the prediction of the shear deformations within the framework of the plastic hinge analysis. This was related to several reasons: The two approaches applied for including the shear deformations in the plastic hinge models were developed for well detailed members which showed only little shear degradation and had constant shear to flexural deformation ratios over the entire displacement ductility range. All of this was not the case for the analysed test units. Both equations depend on the crack angle, which was here taken from photographs. Predicting the crack angle was associated to considerable uncertainties, which render the application of the shear deformation equations difficult for the assessment of wall-type bridge piers. To reliably predict the total force-deformation relationship of such piers, an estimate of the shear deformations must, however, be included when computing the force-deformation response. For this reason, future work will aim at improving the shear deformation estimates, especially with regards to the area over which shear deformation is assumed to spread as well as to the magnitude of those spread deformations. Predictions of the crack angles need to be modified or, since the dependency on the crack angle alone did not yield satisfactory results with regards to the different aspect and reinforcement ratios, the crack angle needs to be replaced by measures which capture these influences better.

ACKNOWLEDGEMENT

The study presented in this paper has been carried out in the framework of a research project funded by the Swiss Federal Roads Office (FEDRO) with project number AGB 2008/001. This financial support is gratefully acknowledged.

REFERENCES

Bentz, E., Vecchio, F. and Collins, M.P. (2006). Simplified modified compression field theory for calculating shear strength of reinforced concrete elements. *ACI Structural Journal*, **103:4**, 614-624.

Beyer, K., Dazio, A. and Priestley, M.J.N. (2008). Seismic design of torsionally eccentric buildings with U-shaped RC walls. Research Report ROSE - 2008/03, ROSE School, Pavia, Italy.

Beyer, K., Dazio, A. and Priestley, M.J.N. (2011). Shear deformations of slender RC walls under seismic loading. *ACI Structural Journal*, **108:2**, 167-177.

Bimschas, M., (2010). Displacement-Based Seismic Assessment of Existing Bridges in Regions of Moderate Seismicity, IBK Report 326, Swiss Federal Institute of Technology ETH, Zurich, Switzerland.

Biskinis, D. and Fardis, M.N. (2010a). Flexure-controlled ultimate deformations of members with continuous or lap-spliced bars. *Structural concrete*, **11:2**, 93-108.

Biskinis, D. and Fardis, M.N. (2010b). Deformations at flexural yielding of members with continuous or lap-spliced bars. *Structural concrete*, **11:3**, 127-138.

Bohl, P. and Adebar, P. (2011). Plastic hinge lengths in high-rise concrete shear walls. ACI Structural Journal, **108:2**, 148-157.

CEN (2004). Eurocode 2: Design of concrete structures - Part 1-1: General rules and rules for buildings. European Committee for Standardization, Brussels, Belgium.

CEN (2005). Eurocode 8: Design of structures for earthquake resistance - Part 3: Assessment and retrofitting of buildings. European Committee for Standardization, Brussels, Belgium.

Collins, M.P. and Mitchell, D. (1991). Prestressed concrete structures. Response publications, Canada.

Dazio, A., Beyer K. and Bachmann, H. (2009). Quasi-static cyclic tests and plastic hinge analysis of RC structural walls. Engineering Structures, **31:7**, 1556-1571.

Hannewald, P., Bimschas M., and Dazio, A. (2012). *To be published*, Quasi-static cyclic tests on RC bridge piers with detailing deficiencies, IBK Report, Swiss Federal Institute of Technology ETH, Zurich, Switzerland.

Hines, E., Restrepo, J. and Seible, F. (2004). Force-displacement charcaterization of well-confined bridge piers. *ACI Structural Journal* **101:4**, 537-548.

Mander, J.B., Priestley, M.J.N, and Park, R. (1988). Theoretical stress-strain model for confined concrete. *ASCE Journal of Structural Engineering*, **114:8**, 1804–1826.

MathWorks. (2010). Matlab, Version R2010b, The MathWorks, Inc., Natick, Massachusetts, U.S.A.

Priestley, M.J.N, Calvi,G.M. and Kowalsky,M.J. (2007). Displacement based seismic design of structures. IUSS Press, Pavia, Italy.